

# New fluorenyl-substituted ditopic dioxotetraamine ligands and their copper(II) complexes—synthesis, crystal structure, magnetic properties and solution behavior†

Qing-Xiang Li,<sup>a,b</sup> Yi-Ning Wang,<sup>a</sup> Qin-Hui Luo,<sup>\*a</sup> Xue-Lei Hu<sup>a,b</sup> and Yi-Zhi Li<sup>a</sup>

Received 23rd November 2007, Accepted 8th February 2008

First published as an Advance Article on the web 18th March 2008

DOI: 10.1039/b717866b

A new fluorenyl-substituted dioxotetraamine salicylaldehyde Schiff-base ligand (L<sup>1</sup>) has been synthesized by the non-template 1 + 2 condensation of ligand 6-(9-fluorenyl)-1,4,8,11-tetraazaundecane-5,7-dione (L) with salicylaldehyde. From reduction of L<sup>1</sup> with an excess of NaBH<sub>4</sub>, a ditopic dioxotetraamine ligand (L<sup>2</sup>) has been obtained. The copper(II) complex of L<sup>1</sup> has been synthesized and its properties were examined by ES-MS and variable-temperature magnetic susceptibility as well as its crystal structure being determined. Detailed studies have been made on solution chemistry of Cu(II) complex of L<sup>2</sup> by pH-potentiometric and fluorometric titration.

## Introduction

Dioxotetraamine ligands possess structures similar to those of oligo-peptides. They are able to form stable complexes with transition metal ions. Their two amide moieties lose hydrogen ions during coordination with divalent metal ions; therefore they are able to stabilize high oxidation states of metal ions in aqueous solution.<sup>1</sup> The dioxotetraamine ligands have attracted interest due to their special coordination properties and practicality.<sup>2–5</sup> For example, copper(II) and zinc(II) complexes of dioxotetraamine ligands are able to recognize small molecules,<sup>6,7</sup> to be used as models of metal enzymes with physiological activity.<sup>8–10</sup> Therefore, they have potential applications in medicine.<sup>11,12</sup>

Recently, research has been devoted to append a luminophore group to the framework of the dioxotetraamine ligands and to explore new fluorescent signaling systems.<sup>13–19</sup> In view of the high quantum yield and long fluorescent lifetime of fluorene, our group had linked fluorenyl as a luminophore to the dioxotetraamine units and obtained a series of water-soluble ligands (for example L).<sup>20,21</sup> In this paper, we modified the ligand L through condensation with salicylaldehyde and obtained a new Schiff-base ligand L<sup>1</sup>. The reduction of ligand L<sup>1</sup> with an excess of NaBH<sub>4</sub> obtained a ditopic dioxotetraamine ligand L<sup>2</sup>. The copper(II) complex of L<sup>1</sup> [Cu<sub>2</sub>(H<sub>2</sub>L<sup>1</sup>)<sub>2</sub>·H<sub>2</sub>O] was synthesized. The crystal structure of the complex shows that the two arms of L<sup>1</sup> are opened and each arm coordinated with different copper(II) to form a Cu(II)–Cu(II) dinuclear entity. A ferromagnetic exchange coupling effect exists in the complex. Detailed studies have been made on solution chemistry of Cu(II) complex of L<sup>2</sup> by pH-potentiometric and fluorometric titration. The results show that Cu<sup>2+</sup> is only coordinated in compartment B and leads to quenching of the fluorescence of

the fluorenyl group; it cannot move to compartment A at a lower pH value.

## Experimental

### Materials

All starting materials were of reagent grade. The ligand 6-(9-fluorenyl)-1,4,8,11-tetraazaundecane-5,7-dione (L) was prepared by the literature method.<sup>20</sup> Copper(II) perchlorate was prepared by adding perchloric acid to the solution of copper(II) carbonate.

### Physical measurements

Elemental analysis was performed using a Perkin-Elmer 240C analytical instrument. IR spectra were measured as KBr discs using a Nicolet 5DX FT-IR spectrophotometer. The electrospray mass spectrum (ES-MS) was determined on a Finnigan LCQ mass spectrograph. The concentration of the samples was about 0.1 mmol dm<sup>-3</sup>, their MeOH solutions were electrosprayed at a flow-rate of 5 × 10<sup>-6</sup> mol min<sup>-1</sup> with a needle voltage of +4.5 kV. The temperature of the heated capillary in the interface is 200 °C and a fused-silica sprayer was used. The mobile phase was an aqueous solution of methanol (1:1 v/v). The samples were run in the positive-ion mode. The UV spectra were measured on a Lambda 35 spectrophotometer. Emission spectra were recorded on an AB2 luminescence spectrometer (excitation wavelength 282 nm) and were all uncorrected with respect to instrument response. The concentrations of the ligand and Cu<sup>2+</sup> ion in spectrophotometric titrations and in fluorimetric titrations were 5.0 × 10<sup>-4</sup> and 5.0 × 10<sup>-5</sup> mol dm<sup>-3</sup>, respectively. The experiments were carried out in dioxane–water solution (3:1, v/v).

### pH titration

The protonation constants of the ligand L<sup>2</sup> and stability constants of its Cu<sup>2+</sup> complex were studied in a dioxane–water solution (3:1 v/v), because L<sup>2</sup> was not dissoluble in aqueous solutions. The pH values were determined by using a Corning pH meter

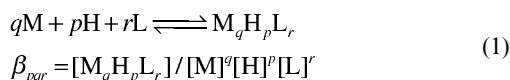
<sup>a</sup>Coordination Chemistry Institute, State Key Laboratory of Coordination Chemistry, Nanjing University, Nanjing, 210093, China. E-mail: qhluo@jlonline.com, lqxwh@yahoo.com

<sup>b</sup>School of Chemical Engineering and Pharmacy, Wuhan Institute of Technology, Hubei Key Lab of Novel Reactor & Green Chemical Technology, Wuhan, 430074, China. E-mail: lqxwh@yahoo.com

†CCDC reference number 666971. For crystallographic data in CIF or other electronic format see DOI: 10.1039/b717866b

with a glass–silver–silver chloride combination electrode with precision  $\pm 0.001$  pH. The electrode was standardized by buffer solutions of potassium hydrogen phthalate and sodium borate. The concentration of  $L^2$  was  $0.0025 \text{ mol dm}^{-3}$  and the molar ratio of  $L^2$  to  $\text{Cu}(\text{NO}_3)_2$  was 1:1. The experimental solutions were titrated with carbonate-free  $0.0825 \text{ mol dm}^{-3}$  NaOH by using a microsyringe with precision  $\pm 2 \mu\text{l}$  under a nitrogen atmosphere in a sealed jacketed vessel at  $25^\circ\text{C}$ . The ionic strength was kept to be  $0.1 \text{ mol dm}^{-3}$  using  $\text{KNO}_3$ .

The equilibria in the systems can be represented by eqn (1):



Where  $q$ ,  $p$ , and  $r$  denote the number of metal ions, hydrogen ions and ligand molecules bound in the complex respectively. A negative  $p$  value shows that a hydrogen ion is released during coordination. The protonation constants of the ligands were calculated by the PKAS program.<sup>22</sup> The equilibrium constants of complexes were calculated by using the program LEMIT,<sup>23</sup> which is based on the Newton–Raphson and Gauss–Newton method for minimizing  $U$  in eqn (2), where  $C_{\text{Hi}}^{\text{calc}}$  and  $C_{\text{Hi}}^{\text{expt}}$  denote the calculated and experimental values of  $\text{H}^+$  concentration at the  $i$ th point.

$$U = \sum_i (C_{\text{Hi}}^{\text{calc}} - C_{\text{Hi}}^{\text{expt}})^2 \quad (2)$$

### Crystal structure determination†

X-Ray intensity data for the binuclear copper(II) complex were collected on a SMART-CCD area-detector diffractometer using graphite monochromatized Mo  $K\alpha$  radiation ( $\lambda = 0.71073 \text{ \AA}$ ). Data reduction and cell refinement were performed by the SMART and SAINT programs.<sup>24</sup> The absorption corrections were carried out by an empirical method. The structure was solved by direct methods (Bruker SHELXTL) and refined on  $F^2$  by full-matrix least-squares (Bruker SHELXTL) using all unique data.<sup>25</sup> The non-H atoms in the structure were subjected to anisotropic refinement. Hydrogen atoms were located geometrically and treated with the riding mode.

### Magnetic properties

The variable-temperature magnetic susceptibility of the binuclear copper(II) complex was measured from 1.88 to 200 K in a magnetic field of 20 kOe using a SQUID magnetometer. Diamagnetic corrections were estimated from Pascal's constants.<sup>26</sup>

### Syntheses of the complexes

**$L^1$ .** 6-(9-Fluorenyl)-1,4,8,11-tetraazaundecane-5,7-dione ( $L$ ) (1.76 g, 5 mmol) was dissolved in absolute ethanol (200 ml) under reflux conditions. A solution of salicylaldehyde (1.46 g, 12 mmol) in absolute ethanol (50 ml) was then added dropwise. After stirring for 4 h, the mixture was cooled and filtered, washed with ethanol and dried in a vacuum desiccator; a yellow powder precipitate ( $L^1$ ) was obtained. Yield: 1.50 g (53.6%). Found: C, 72.29; H, 6.25; N, 10.48%.  $\text{C}_{34}\text{H}_{32}\text{N}_4\text{O}_4$  requires: C, 72.84; H, 5.75; N, 9.99%. IR(KBr  $\text{cm}^{-1}$ ): 3294 (s, (NH, OH)); 3062, 2930, 2862 (m, (CH)); 1666 (vs, (CO)); 1636 (vs (N=C)); 756–729 (m, (CH)).

**$L^2$ .**  $L^1$  (0.112 g, 0.20 mmol) suspended in absolute methanol (100 ml) was treated with an excess of  $\text{NaBH}_4$  in batches at  $0^\circ\text{C}$ , and the resultant solution was stirred for 48 h and then filtered. The precipitate was washed with methanol. The washed liquid and the filtrate were merged, the solvent was removed by rotary evaporation to give yellow oily residue and water was added to produce a light-yellow precipitate. The precipitate was washed with large amount of water and dried; after recrystallization with methanol, a yellow powder solid of  $L^2$  was obtained. Yield: 1.00 g (66.2%). Found: C, 72.99; H, 6.58; N, 9.92%.  $\text{C}_{34}\text{H}_{32}\text{N}_4\text{O}_4$  requires: C, 72.32; H, 6.43; N, 9.92%. IR(KBr  $\text{cm}^{-1}$ ): 3291 (s, (NH, OH)); 3065, 2930, 2849 (m, (CH)); 1665 (vs, (CO)); 756–729 (m, (CH)).

**$[\text{Cu}_2(\text{H}_2L^1)_2] \cdot \text{H}_2\text{O}$ .**  $L^1$  (0.112 g, 0.20 mmol) suspended in acetonitrile–methanol (7:3 v/v) (30 ml) was added dropwise to 0.074 g (0.20 mmol) of copper(II) perchlorate in 3 ml methanol solution. After stirring and refluxing for 30 min, during which time sodium hydroxide (0.070 g, 1.75 mmol) was added to the mixture in batches to keep its pH at 9, the mixture was cooled and filtered. The dark-green powder solid was isolated after concentration of the filtrate under reduced pressure. Yield: 0.163 g (63%). Found: C, 62.79; H, 5.41; N, 8.61%.  $\text{C}_{68}\text{H}_{66}\text{N}_8\text{O}_{11}\text{Cu}_2$  requires: C, 62.90; H, 5.12; N, 8.63%. IR(KBr  $\text{cm}^{-1}$ ): 3305 (s, (NH, OH)); 3053, 2930, 2862 (m, (CH)); 1642 (vs, (CO)); 1622 (vs (N=H/C)); 758–729 (m, (CH)).  $\Lambda_m$  ( $\text{CH}_3\text{OH}$ , 298.2 K)  $56.30 \text{ S cm}^2 \text{ mol}^{-1}$ . Single crystals suitable for X-ray diffraction analysis† were obtained by slow evaporation of the mother liquor for one week.

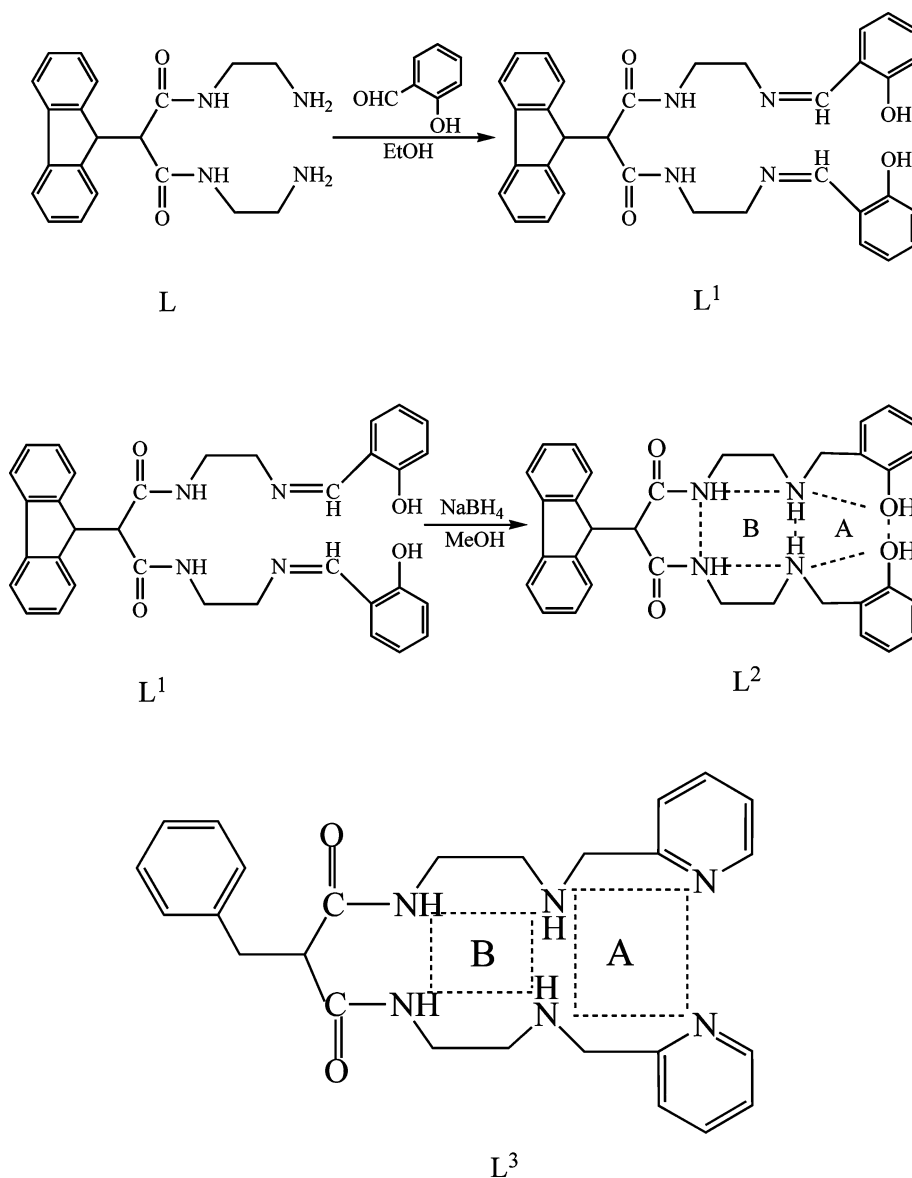
## Results and discussion

### Syntheses and characterization of the compounds

A new dioxotetraamine salicylaldehyde Schiff-base ligand  $L^1$  has been synthesised by condensation of ligand 6-(9-fluorenyl)-1,4,8,11-tetraazaundecane-5,7-dione ( $L$ ) with salicylaldehyde. By reduction of ligand  $L^1$  with an excess of  $\text{NaBH}_4$ , a two-compartment dioxotetraamine ligand  $L^2$  has been obtained. The synthetic routes of ligands are summarized in Scheme 1. A novel binuclear copper(II) complex of ligand  $L^1$  has been obtained. The IR data of the ligands and the copper(II) complex of ligand  $L^1$  are compared in Table 1. From Table 1 it can be seen that all the compounds have strong bands at the range of 756–729  $\text{cm}^{-1}$  which are designated to skeleton stretching of the aromatic ring. The strong peaks near 1665  $\text{cm}^{-1}$  of the compounds are characteristic of the vibration of C=O. The strong bands at about 1630  $\text{cm}^{-1}$  of ligand  $L^1$  and its copper(II) complex are designated to stretching vibration of  $-\text{C}=\text{N}-$ . The strong bands near 3294  $\text{cm}^{-1}$  are due to N–H and O–H stretching vibration of the compounds. The bands of the three compounds at the range of 2849–3065  $\text{cm}^{-1}$  are due to C–H stretching vibration. The low value of molar conductivity implies the copper(II) complex of ligand  $L^1$  is neutral.

### Electrospray mass spectra (ES-MS)

The ES-MS spectra of  $L^1$ ,  $L^2$  and  $[\text{Cu}_2(\text{H}_2L^1)_2] \cdot \text{H}_2\text{O}$  in MeOH solution are shown in Fig. 1, 2 and 3 respectively. The assignments of peaks are listed in Table 2. From Table 2 it can be seen that the ligands  $L^1$  and  $L^2$  not only caught protons in the solution, forming protonated species  $[L^1 + \text{H}^+]^+$  and  $[L^2 + \text{H}^+]^+$  with high abundance, but also were able to bind  $\text{Na}^+$ , forming adducts  $[L^1 + \text{Na}^+]^+$ ,



**Scheme 1** The synthetic route of ligands (L<sup>3</sup>: reported ligand)

**Table 1** IR spectra data of the compounds

Compound	$\nu_{\text{NH}}/\text{cm}^{-1}$	$\nu_{\text{CH}}/\text{cm}^{-1}$	$\nu_{\text{CO}}/\text{cm}^{-1}$	$\nu_{\text{CN}}/\text{cm}^{-1}$	$\nu_{\text{CH}}/\text{cm}^{-1}$
L <sup>1</sup>	3291	3062, 2930, 2862	1666	1636	756–729
L <sup>2</sup>	3294	3065, 2930, 2849	1665	—	756–729
[Cu <sub>2</sub> (H <sub>-2</sub> L <sup>1</sup> ) <sub>2</sub> ·H <sub>2</sub> O]	3305	3053, 2930, 2862	1642	1622	758–729

[2L<sup>1</sup> + Na<sup>+</sup>]<sup>+</sup> and [L<sup>2</sup> + Na<sup>+</sup>]<sup>+</sup> (Na<sup>+</sup> is present in trace amounts in this ligand). The ES mass spectrum of [Cu<sub>2</sub>(H<sub>-2</sub>L<sup>1</sup>)<sub>2</sub>·H<sub>2</sub>O] in the solution is shown in Fig. 3. There are three species [Cu<sub>2</sub>(H<sub>-2</sub>L<sup>1</sup>)<sub>2</sub> + Na<sup>+</sup>]<sup>+</sup>, [Cu<sub>2</sub>(H<sub>-2</sub>L<sup>1</sup>)<sub>2</sub> + K<sup>+</sup>]<sup>+</sup> and [Cu<sub>2</sub>(H<sub>-2</sub>L<sup>1</sup>)<sub>2</sub>-e]<sup>+</sup> which indicate that this complex also exists as a dimer in solution.

### Crystal structure

The crystal data of complex [Cu<sub>2</sub>(H<sub>-2</sub>L<sup>1</sup>)<sub>2</sub>] (Scheme 2) are listed in Table 3. The chemical structure and crystal structure are shown

in Scheme 2 and Fig. 4. The selected bond lengths and angles of complex [Cu<sub>2</sub>(H<sub>-2</sub>L<sup>1</sup>)<sub>2</sub>] are given in Table 4. From Scheme 2, Fig. 4 and Table 4 it can be seen that it is different with our anticipation, two arms of L<sup>1</sup> are opened and each arm coordinated with different copper(II), by means of cross coordinated to form a Cu(II)–Cu(II) dinuclear entity (the atoms that coordinated with copper(II) are nitrogen atoms of Schiff-base and oxygen atoms of phenol hydroxyl). Cu(1) and Cu(2) are located in the center of a slightly distorted square consisted by N(1), N(8), O(1), O(2) (plane 1) and N(4), N(5), O(3), O(4) (plane 2) respectively. Cu(1)

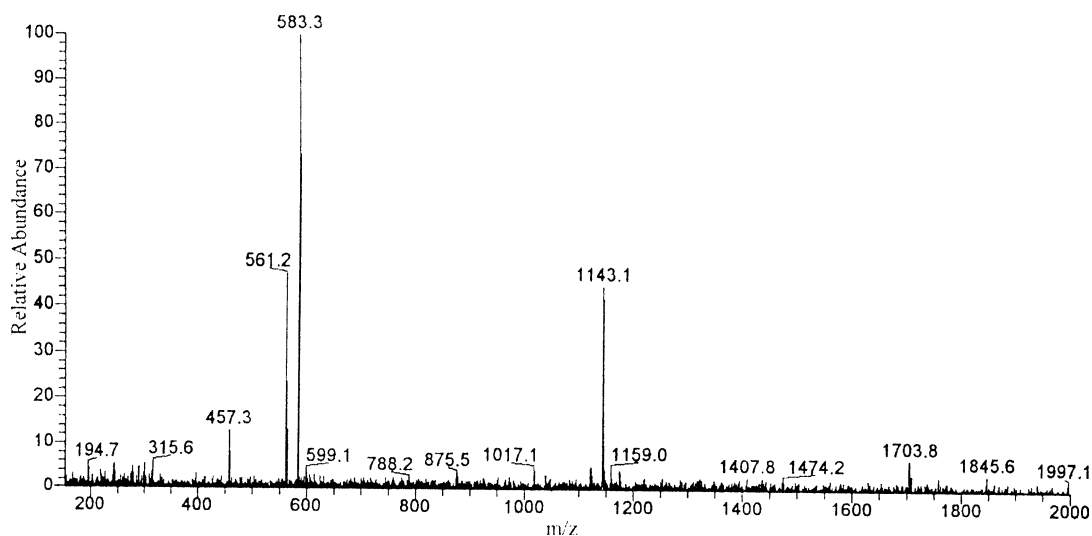


Fig. 1 ES-MS of  $L^1$  in methanol.

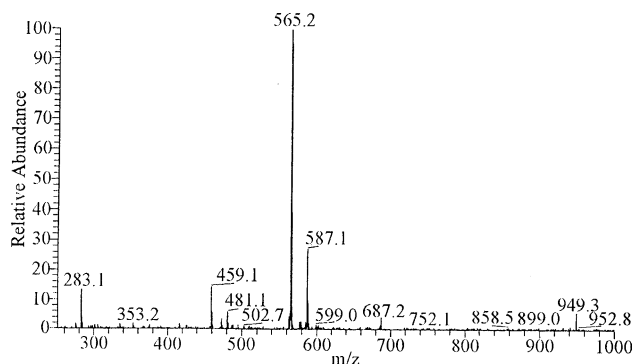


Fig. 2 ES-MS of  $L^2$  in methanol.

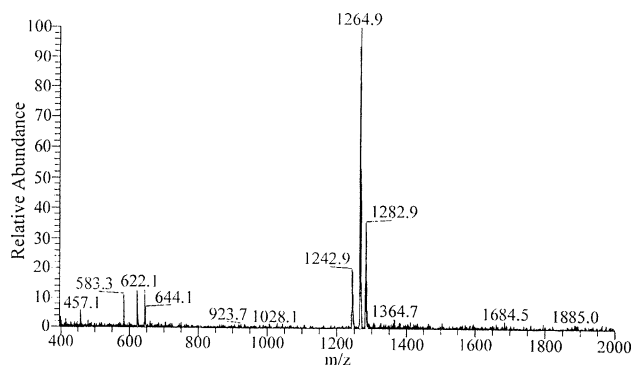
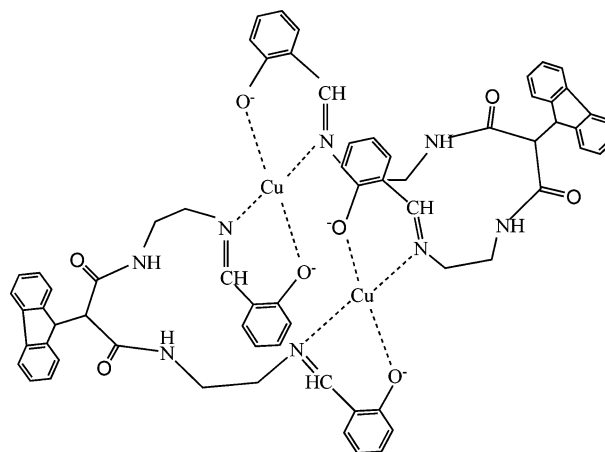


Fig. 3 ES-MS of  $[Cu_2(H_2L^1)_2] \cdot H_2O$  in methanol.

Table 2 The assignments of ES-MS peaks for the compounds in methanol

Compound	Peak (m/z) <sup>a</sup>	Species
$L^1$	583.3 (100)	$[L^1 + Na^+]^+$
	561.2 (48)	$[L^1 + H^+]^+$
	1143.1 (47)	$[2L^1 + Na^+]^+$
$L^2$	565.2 (100)	$[L^2 + H^+]^+$
	587.1 (30)	$[L^2 + Na^+]^+$
$[Cu_2(H_2L^1)_2] \cdot H_2O$	1264.9 (100)	$[Cu_2(H_2L^1)_2 + Na^+]^+$
	1282.9 (36)	$[Cu_2(H_2L^1)_2 + K^+]^+$
	1242.9 (20)	$[Cu_2(H_2L^1)_2 - e]^+$

<sup>a</sup> Relative abundance is given in the parentheses.



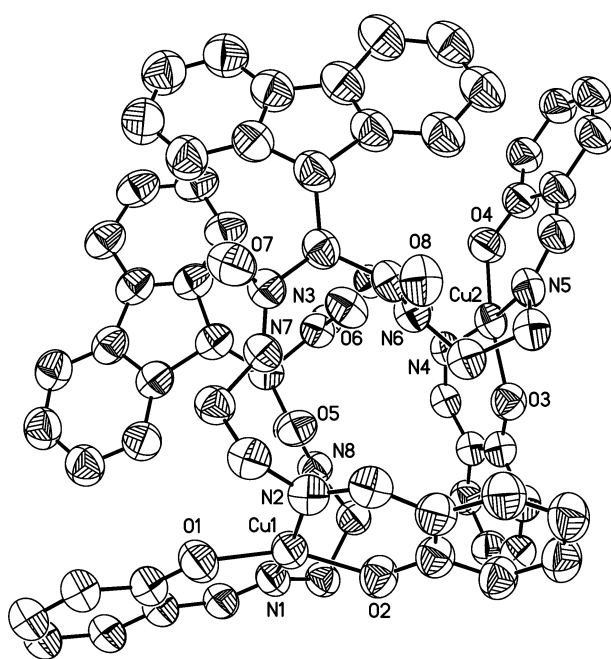
Scheme 2 Chemical structure of  $[Cu_2(H_2L^1)_2]$ .

atom is 0.0937 Å out of plane 1 and Cu(2) atom is 0.0043 Å out of plane 2. In the two planes, the average bond lengths of Cu–N are 1.971 and 2.010 Å respectively, slightly longer than that of Cu–O (1.864, 1.909 Å), indicating that the oxygen atoms have stronger ability to coordinate to copper(II) than that of nitrogen atoms. In plane 1, the O(1)–Cu(1)–N(1), O(2)–Cu(1)–N(1), O(2)–Cu(1)–N(8), O(1)–Cu(1)–N(8) angles are 93.41(12), 90.44(12), 92.75(12) and 89.35(12)° respectively, which are close to 90°. In plane 2,

the O(3)–Cu(2)–N(5), O(4)–Cu(2)–N(5), O(4)–Cu(2)–N(4), O(3)–Cu(2)–N(4) angles [89.77(11), 91.55(11), 88.66(11) and 91.71(11)° respectively] are also close to 90°. The separation between the two metals is 7.435 Å. The dihedral angle between plane 1 and plane 2 is 81.3°, so the planes are approximately perpendicular. The dihedral angle between two fluorenyl group planes is 14.8° so they

**Table 3** Crystal data of  $[\text{Cu}_2(\text{H}_2\text{L}^1)]_2 \cdot \text{H}_2\text{O}$ 

Formula	$\text{C}_{68}\text{H}_{62}\text{Cu}_2\text{N}_8\text{O}_9$
M	1262.34
Crystal system	Monoclinic
Space group	$P2_1/n$
$a/\text{\AA}$	13.749(2)
$b/\text{\AA}$	19.026(3)
$c/\text{\AA}$	24.307(4)
$\beta/^\circ$	92.51(1)
$U/\text{\AA}^3, Z$	6352.3(17), 4
$2\theta$ range/ $^\circ$	3.40–50.00
T/K	293(2)
$\mu(\text{Mo K}\alpha)/\text{mm}^{-1}$	0.732
Reflections collected	31183
Independent reflections	11138
R(int)	0.033
Observed data [ $I > 2\sigma(I)$ ]	5989
S	1.03
Final R1, wR2 [ $I > 2\sigma(I)$ ]	0.0420, 0.1109
(all data)	0.0892, 0.1168

**Fig. 4** Crystal structure of  $[\text{Cu}_2(\text{H}_2\text{L}^1)]_2 \cdot \text{H}_2\text{O}$ .**Table 4** Selected bond distances ( $\text{\AA}$ ) and angles ( $^\circ$ ) of  $[\text{Cu}_2(\text{H}_2\text{L}^1)]_2 \cdot \text{H}_2\text{O}$ 

Cu(1)–N(1)	1.958(3)	Cu(2)–O(3)	1.914(2)
Cu(1)–N(8)	1.984(3)	Cu(2)–O(4)	1.904(2)
Cu(1)–O(1)	1.867(2)	C(7)–N(1)	1.257(4)
Cu(1)–O(2)	1.860(2)	C(14)–N(8)	1.248(4)
Cu(2)–N(4)	1.999(3)	C(21)–N(4)	1.303(4)
Cu(2)–N(5)	2.020(3)	C(28)–N(5)	1.283(4)
O(1)–Cu(1)–N(1)	93.41(12)	O(3)–Cu(2)–N(5)	89.78(11)
O(2)–Cu(1)–N(1)	90.44(11)	O(4)–Cu(2)–N(5)	91.53(12)
O(2)–Cu(1)–N(8)	92.75(12)	O(4)–Cu(2)–N(4)	88.67(11)
O(1)–Cu(1)–N(8)	89.35(12)	O(3)–Cu(2)–N(4)	91.71(11)
O(1)–Cu(1)–O(2)	154.16(11)	O(3)–Cu(2)–O(4)	169.62(11)
N(1)–Cu(1)–N(8)	166.66(11)	N(4)–Cu(2)–N(5)	170.62(11)

are close to parallel. The dihedral angle between two fluorenyl group planes with plane 1 are 87.5 and 75.2 $^\circ$  respectively, and with plane 2 are 66.1 and 56.8 $^\circ$  respectively. This makes the whole

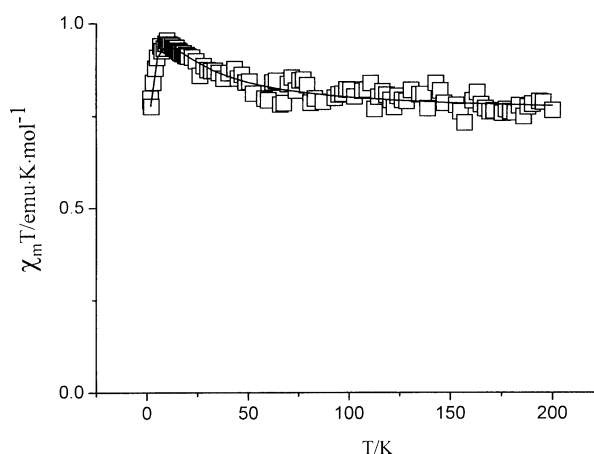
molecule form a similar open cuboid structure. Plane 1, plane 2 and two fluorenyl group planes constituted the four faces of the cuboid.

### Magnetic properties

The solid-state magnetic susceptibilities of  $[\text{Cu}_2(\text{H}_2\text{L}^1)]_2 \cdot \text{H}_2\text{O}$  was measured from 1.88 to 200 K. The temperature ( $T$ ) dependence of  $\chi_m T$  (product of molar magnetic susceptibility and temperature) is shown in Fig. 5. The  $\chi_m T$  is 0.76 emu K/mol at 200K, increases with decreasing temperature to a maximum of 0.95 emu K/mol at 10.00 K due to a ferromagnetic exchange coupling and then  $\chi_m T$  decreases sharply down to 1.88 K. The experimental data can be fitted by the following expression:<sup>27</sup>

$$\chi_m = \frac{2N\beta^2 g^2}{k(T-\theta)} [3 + \exp(-J/kT)]^{-1} \quad (3)$$

where  $\beta$  and  $\kappa$  have the normal meanings,  $J$  denotes an intra-dimer exchange integral and  $\theta$  is the Curie–Weiss correction which corrects the effective inter-dimer exchange. By fitting eqn (3) we obtained  $g = 2.003$ ,  $J = 21.30 \text{ cm}^{-1}$ ,  $\theta = -0.55 \text{ cm}^{-1}$ ,  $R = 3.7 \times 10^{-4}$  ( $R = \sum_i [(\chi_m T)_{\text{obs}}(i) - (\chi_m T)_{\text{calc}}(i)]^2 / \sum_i [(\chi_m T)_{\text{obs}}(i)]^2$ ,  $i$  denotes the number of experimental points). The results indicate that despite the large separation between the two Cu(II) (7.435  $\text{\AA}$ ), the intra-molecular ferromagnetic exchange coupling is still exist. The increase of  $\chi_m T$  with increase of temperature results from this exchange coupling. This is due to the fact that two planes which contain Cu(II) are approximately vertical and the of two Cu(II) are also approximately vertical; the super exchange effect which causes the intra-molecular ferromagnetic exchange coupling exists between the two metals.<sup>28</sup>

**Fig. 5** Plot of  $\chi_m T$  vs.  $T$  for  $[\text{Cu}_2(\text{H}_2\text{L}^1)]_2 \cdot \text{H}_2\text{O}$ . (—) The fitting curve, ( $\square$ ) experimental data.

### Stability of the complex

The titration curves of ligand  $\text{L}^2$  in the absence and presence of copper ions are shown in Fig. 6, from which it can be seen that each curve has two steps with defined inflection points. The first steps of both curves are at about  $a = 1$  ( $a$  denotes the number of equivalents of NaOH per mole of ligand), corresponding to the free strong acid being neutralized. For curve 2, the second step is at about  $a = 4$ –5, indicating the formation of species

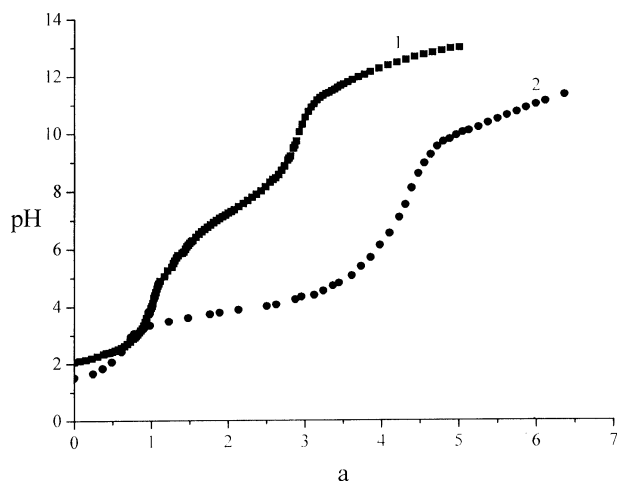


**Fig. 6** pH titration curves in dioxane–water solution (3:1 v/v),  $I = 0.1 \text{ mol dm}^{-3}$  ( $\text{KNO}_3$ ),  $25^\circ\text{C}$ . The concentrations, (1)  $[\text{L}^2] = 0.00521 \text{ mol dm}^{-3}$ ,  $[\text{HNO}_3] = 0.0992 \text{ mol dm}^{-3}$ ; (2)  $[\text{L}^2] = [\text{Cu}^{2+}] = 0.00516 \text{ mol dm}^{-3}$ ,  $[\text{HNO}_3] = 0.0992 \text{ mol dm}^{-3}$ .

**Table 5** Logarithm of equilibrium constants<sup>a</sup> at  $25 \pm 0.01^\circ\text{C}$ ,  $I = 0.1 \text{ mol dm}^{-3}$  ( $\text{KNO}_3$ ) in dioxane–water solution (3:1 v/v)

Reaction	$\text{H}^+$	$\text{Cu}^{2+}$
$\text{H}^+ + \text{L}^2 \rightleftharpoons [\text{HL}^2]^+$	$8.19 \pm 0.02$	
$2\text{H}^+ + \text{L}^2 \rightleftharpoons [\text{H}_2\text{L}^2]^{2+}$	$14.42 \pm 0.02$	
$\text{Cu}^{2+} + \text{L}^2 \rightleftharpoons [\text{CuL}^2]^{2+}$		$9.56 \pm 0.02$
$\text{Cu}^{2+} + \text{L}^2 \rightleftharpoons [\text{CuH}_1\text{L}^2]^+ + \text{H}^+$		$5.04 \pm 0.03$
$\text{Cu}^{2+} + \text{L}^2 \rightleftharpoons [\text{CuH}_2\text{L}^2] + 2\text{H}^+$		$-3.50 \pm 0.02$
$\log U$		$-6.38$

<sup>a</sup> For each system, titrations were performed twice and during each titration more than 60 points were recorded.

$[\text{CuH}_1\text{L}^2]^+$  and  $[\text{CuH}_2\text{L}^2]$ . Assuming the coexistence of  $[\text{Cu}^{2+}]$ ,  $[\text{CuL}^2]^{2+}$ ,  $[\text{CuH}_1\text{L}^2]^+$  and  $[\text{CuH}_2\text{L}^2]$ , the equilibrium constants were obtained by the curve fitting. The equilibrium constants of the species are listed in Table 5. The distribution curves of the species calculated by equilibrium constants are shown in Fig. 7.

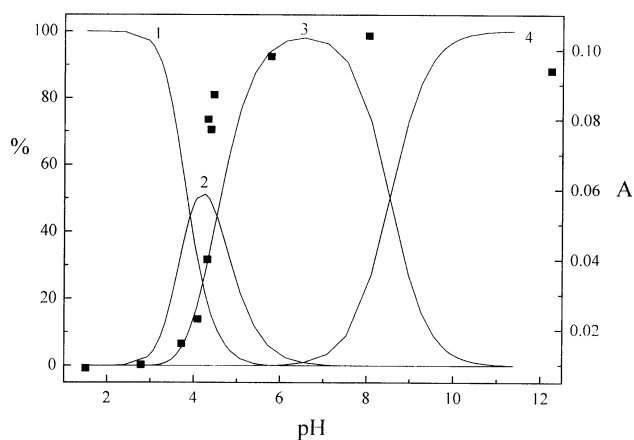


**Fig. 7** Species distribution for curve 2 in Fig. 6 and dependence of the absorbance  $A$  (■) on the pH for the  $\text{L}^2 + \text{Cu}^{2+}$  system. Species: 1.  $\text{Cu}^{2+}$ ; 2.  $[\text{CuL}^2]^{2+}$ ; 3.  $[\text{CuH}_1\text{L}^2]^+$ ; 4.  $[\text{CuH}_2\text{L}^2]$ .

From Fig. 7 it can be seen that  $[\text{CuH}_1\text{L}^2]^+$  is the predominant species and its percentage is above 90% at pH 6–7.

### Sensing properties of the complexes

In Fig. 8 the fluorescence emission spectrum of the ligand  $\text{L}^2$  in dioxane–water solution (3:1 v/v) is shown. The maximum fluorescence emission is located at 308 nm (pH = 9.0) by excitation of 282 nm. The intensity and position of the maximum emission remains constant when the pH changes, implying that protonation of the ligand  $\text{L}^2$  ( $[\text{HL}^2]^+$ ,  $[\text{H}_2\text{L}^2]^{2+}$ ) has little influence on the fluorescence intensity. During titration of an acidic dioxane–water solution (3:1 v/v) of  $\text{L}^2$  containing an equivalent of  $\text{Cu}^{2+}$  ion with  $\text{NaOH}$ , with the coordination of copper(II) ion, the fluorescence intensity of the solution decreases at about pH 3, and almost complete fluorescence quenching is observed at pH 6. The change in fluorescence emission spectrum with pH was shown in Fig. 9.

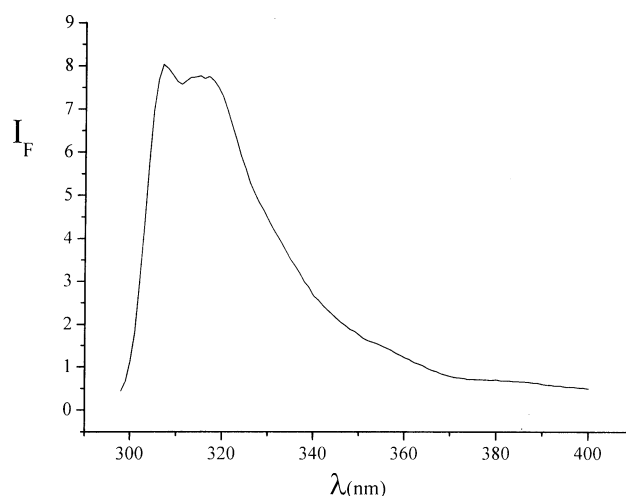


**Fig. 8** Fluorescence emission of ligand  $\text{L}^2$  in dioxane–water solution (3:1 v/v) ( $5.0 \times 10^{-5} \text{ mol dm}^{-3}$ , pH = 9.0) with excitation at 282 nm and an excitation slit width of 5 nm.

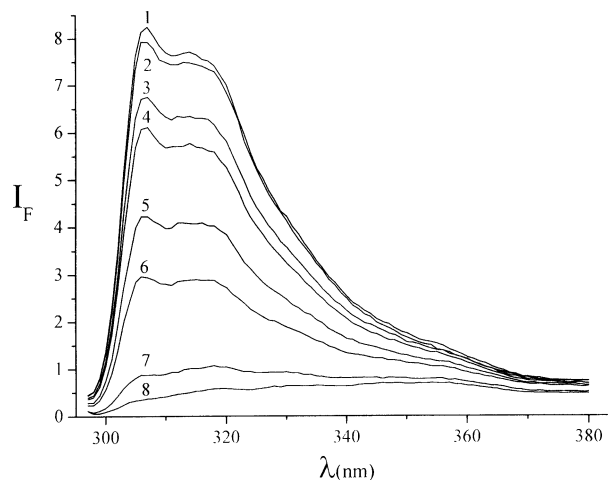


**Fig. 9** The change in fluorescence emission with pH for a dioxane–water solution (3:1 v/v) containing  $\text{L}^2$  plus 1 equiv.  $\text{Cu}^{2+}$  ions ( $c = 5.0 \times 10^{-5} \text{ mol dm}^{-3}$ , from 1 to 8, the pH values are 1.51, 2.79, 3.72, 4.09, 4.31, 4.42, 5.80 and 12.24 respectively) with excitation at 282 nm and an excitation slit width of 5 nm.

The dependence of fluorescence intensity  $I_F$  (■) ( $\lambda_{em} = 308$  nm) on the pH was shown in Fig. 10. The plot of fluorescence intensity  $I_F$  versus pH displays a typical sigmoidal curve.

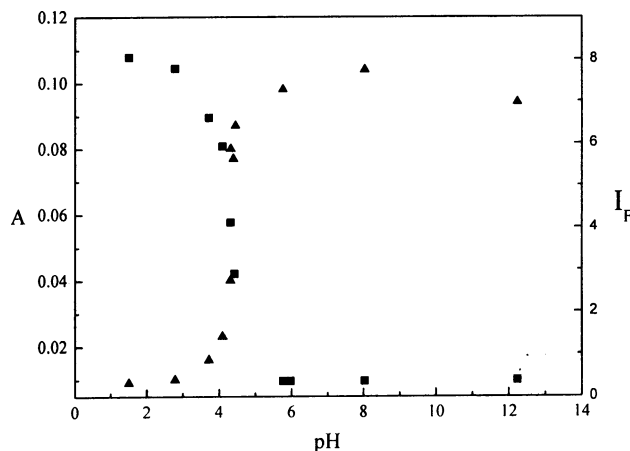


**Fig. 10** The dependence of fluorescence intensity  $I_F$  (■) ( $\lambda_{em} = 308$  nm) and absorbance  $A$  (▲) ( $\lambda = 601$  nm) on the pH for a dioxane–water solution (3:1 v/v) containing  $L^2$  plus 1 equiv.  $Cu^{2+}$  ions.

For studying the quenching mechanism, an analogous spectrophotometric titration experiment was performed. On addition of base, the color of the solution becomes purple; the d–d absorption band of  $Cu^{2+}$  shifting from 830 nm to 601 nm, the absorption band at 601 nm develops and reaches its maximum value at about pH 6.00; at this pH the solution is almost complete fluorescence quenching. The plot of absorbance  $A$  versus pH (▲ in Fig. 10) shows a sigmoidal curve shape too, which is symmetrical to the  $I_F$ /pH profile and centered at the same pH (pH  $\approx$  4.30). The dependence of the absorbance  $A$  on the pH is contrary to that of the fluorescence intensity. The curve of  $A$  vs. pH can be conveniently superimposed on the distribution diagram of  $[CuH_{-1}L^2]^+$  (Fig. 7, curve 3). This indicates that the absorption band at 601 nm is caused by the  $Cu^{2+}$  d–d jump of species  $[CuH_{-1}L^2]^+$ , and that the formation of  $[CuH_{-1}L^2]^+$  leads to quenching the fluorescence.

Making a comparison between the ultraviolet spectrum of  $L^2 + Cu^{2+}$  (1:1) (pH = 3.35) and that of  $Cu(NO_3)_2$  aqueous solution, we find the absorption band at 830 nm of  $L^2 + Cu^{2+}$  (1:1) (pH = 3.35) is very similar to that of  $Cu(NO_3)_2$  aqueous solution. Moreover, the mass spectrum (ES-MS) of an acidic solution of  $L^2 + Cu^{2+}$  (1:1) (pH = 3.72) demonstrates that  $[L^2 + H]^+$  is a main species [ $m/z$  (%) = 565.1 (100)], and the peak of complex [ $m/z$  (%) = 625.9 (< 5)] is very weak. But when the pH is adjusted to 5.80,  $[CuH_{-1}L^2]^+$  become a main species [ $m/z$  (%) = 625.9 (55)]. It is therefore suggested that in an acid solution the absorption band at 830 nm is caused by the d–d jump of hydrated  $Cu^{2+}$ . Namely, in a lower pH the complexes were almost not formed, they were formed with the pH increasing. Contrasting the ultraviolet spectrum of complexes with that of the reported ditopic dioxotetraamine ligand  $L^3$  (Scheme 1),<sup>17</sup> we find the ultraviolet spectrum of complexes (601 nm) are close to that of  $[CuH_{-2}L^3]^+$  (590 nm), in which the  $Cu^{2+}$  is coordinated in compartment B. It is therefore suggested that in  $L^2$  the  $Cu^{2+}$  is only coordinated in compartment B and leads to quenching of the fluorescence of the fluorenyl group; it cannot move to compartment A at a lower pH value.

## Conclusion

Two new fluorenyl-substituted multidentate ligands  $L^1$  and  $L^2$  were prepared. The two ligands showed very different coordination chemistry toward the  $Cu(II)$  ion. A dimeric species  $[Cu_2(H_{-2}L^1)_2]$  was isolated when the Schiff base  $L^1$  was treated with  $Cu(II)$  ions in the presence of NaOH. The dimeric nature of the complex was supported by the X-ray crystal structure determined† and ES-MS data. Structural analysis revealed that the  $Cu(II)$  ions coordinated to the outer N atom and O atom of the two Schiff base and leaving the inner N4 compartment of  $L^1$  unoccupied. The solid-state variable temperature magnetic susceptibility studies showed the existence of intra-molecular ferromagnetic exchange coupling between the two  $Cu(II)$  centers.

The interaction of  $Cu(II)$  with  $L^2$  was examined by pH-potentiometric titration and ES-MS. Results showed that at pH 5.8, the main species in solution was a monomeric species  $[CuH_{-1}L^2]^+$ . Absorption spectroscopy suggested that  $Cu(II)$  only coordinated to the inner N4 compartment of  $L^2$ . Fluorometric titration indicated that  $Cu(II)$  ions quenched the fluorescence of the  $L^2$  ligand.

## Acknowledgements

This project was supported by the National Natural Science Foundation of China (20571058).

## References

- M. Kodama and E. Kimura, *J. Chem. Soc., Dalton Trans.*, 1981, 694.
- (a) E. Kimura, *Pure Appl. Chem.*, 1986, **58**, 1461; (b) E. Kimura, *Pure Appl. Chem.*, 1989, **61**, 823; (c) X. H. Bu, D. L. An, X. C. Cao, R. H. Zhang, C. Thomas and E. Kimura, *J. Chem. Soc., Dalton Trans.*, 1998, 2247; (d) X. H. Bu, X. C. Cao, D. L. An, R. H. Zhang, C. Thomas and E. Kimura, *J. Chem. Soc., Dalton Trans.*, 1998, 433.
- E. Kimura, in *Crown Compounds toward Future Application*, ed. S. R. Cooper, VCH, New York, 1992, ch. 6.
- (a) G. E. Jackson, P. W. Linder and A. Voye, *J. Chem. Soc., Dalton Trans.*, 1996, 4605; (b) X. H. Bu, D. L. An, Y. T. Chen, M. Shionoya and E. Kimura, *J. Chem. Soc., Dalton Trans.*, 1995, 2289; (c) X. H. Bu, Z. H. Zhang, D. L. An, Y. T. Chen, M. Shionoya and E. Kimura, *Inorg. Chim. Acta*, 1998, **249**, 125; (d) M. Kodama, T. Koike and E. Kimura, *Bull. Chem. Soc. Jpn.*, 1995, **68**, 1627.
- Q. H. Luo, S. R. Zhu, M. C. Shen, S. Y. Yu, Z. Zhang, X. Y. Huang and Q. J. Wu, *J. Chem. Soc., Dalton Trans.*, 1994, 1873.
- M. Shionoya, T. Ikeda, E. Kimura and M. Shiro, *J. Am. Chem. Soc.*, 1994, **116**, 3848.
- (a) E. Kimura, T. Ikeda and M. Shionoya, *Pure Appl. Chem.*, 1997, **69**, 2187; (b) E. Kimura, M. Sasada, M. Shionoya, T. Koike, H. Kurosaki and M. Shiro, *J. Bio. Inorg. Chem.*, 1997, 74.
- E. Kimura, in *Progress in Inorganic Chemistry*, K. D. Karlin, Wiley, 1994, vol. 41, p. 443.
- E. Kimura, *Pure Appl. Chem.*, 1993, **65**, 355.
- (a) Q. H. Luo, C. J. Feng, S. R. Zhu, M. C. Shen, A. D. Liu, H. C. Gu, F. M. Li and S. J. Di, *Radiat. Phys. Chem.*, 1998, **53**, 397; (b) J. J. Zhang, Q. H. Luo, D. L. Long, J. T. Chen, F. M. Li and A. D. Liu, *J. Chem. Soc., Dalton Trans.*, 2000, 1893.
- M. Shionoya, E. Kimura and M. Shiro, *J. Am. Chem. Soc.*, 1993, **115**, 6730.
- Y. P. Tian, Y. Z. Fang, Q. H. Luo, M. C. Shen, Q. Lu and W. M. Shen, *Free Radical Biol. Med.*, 1992, **13**, 533.
- L. Fabbriizzi and A. Poggi, *Chem. Soc. Rev.*, 1995, 197.
- L. Fabbriizzi, M. Licchelli, P. Pallavicini, D. Sacchi and A. Taglietti, *Analyst*, 1996, **121**, 1763.
- L. Fabbriizzi, M. Licchelli, P. Pallavicini, A. Perotti and D. Sacchi, *Angew. Chem., Int. Ed. Engl.*, 1994, **33**, 1975.

- 16 V. Amendola, L. Fabbrizzi, C. Mangano, P. Pallavicini, A. Perotti and A. Taglietti, *J. Chem. Soc., Dalton Trans.*, 2000, 185.
- 17 V. Amendola, C. Brusoni, L. Fabbrizzi, C. Mangano, H. Miller, P. Pallavicini, A. Perotti and A. Taglietti, *J. Chem. Soc., Dalton Trans.*, 2001, 3528.
- 18 V. Amendola, L. Fabbrizzi, C. Mangano, H. Miller, P. Pallavicini, A. Perotti and A. Taglietti, *Angew. Chem., Int. Ed.*, 2002, **14**, 2553.
- 19 P. Pallavicini, G. Dacarro, C. Mangano, S. Patroni, A. Taglietti and R. Zaroni, *Eur. J. Inorg. Chem.*, 2006, **22**, 4649.
- 20 L. J. Jiang, Q. H. Luo, C. Y. Duan, M. C. Shen, H. W. Hu and Y. J. Liu, *Inorg. Chim. Acta*, 1999, **295**, 48.
- 21 L. J. Jiang, Q. H. Luo, Q. X. Li, M. C. Shen and H. W. Hu, *Eur. J. Inorg. Chem.*, 2002, 664.
- 22 A. E. Martell, and R. J. Motekaitis, *Determination and Use of Stability Constants*, VCH Publishers, New York, 2nd edn, 1992, p. 129.
- 23 (a) J.-J. Zhang, Q.-H. Luo, D.-L. Long, J.-T. Chen, F.-M. Li and A.-D. Liu, *J. Chem. Soc., Dalton Trans.*, 2000, 1893; (b) Q.-H. Luo, M.-C. Shen, Y. Ding, X.-L. Bao and A.-B. Dai, *Talanta*, 1990, **37**, 357.
- 24 *SMART and SAINT. Area detector control and integration software*, Siemens Analytical X-Ray Systems, Inc., Madison, Wisconsin, USA, 1996.
- 25 G. M. Sheldrick, *SHELXTL V5.1*, Bruker AXS, Inc., Madison, Wisconsin, USA, 1997.
- 26 O. Kahn, *Molecular Magnetism*, VCH Publishers, Inc., New York, 1993.
- 27 S. Sikorav, I. B. Waksman and O. Kahn, *Inorg. Chem.*, 1984, **23**, 490.
- 28 R. L. Carlin, *Magnetochemistry*, Springer-Verlag, Berlin Heidelberg, 1986.